Check for updates

ORIGINAL ARTICLE

Application of MINICS software in measuring parameters of femoral neck fractures and its clinical significance

Aplicación del software MINICS en la medición de los parámetros de las fracturas del cuello femoral y su importancia clínica

Feng Liu, Peng Su, Lichao Zhang, Yi Zhang, and Ruyi Zhang*

Department of Orthpedics, Beijing Shijingshan Hospital, Beijing, China

Abstract

Objective: *This study aimed to investigate the application of MIMICS software in measuring femoral neck fracture (FNF) parameters and its clinical significance.* **Method:** *Computed tomography data from 72 patients with FNFs were used to reconstruct three-dimensional (3D) models using MIMICS. The FNFs were divided into valgus and bowing groups based on the coronal femoral head-neck angle. A simulated sphere identified the center of the femoral head, and a 3D coordinate system was established. Statistical analyses were performed.* **Results:** *The valgus group showed more lateral x-axis and upward z-axis displacement (both $p < 0.01$). The medial x-axis and downward z-axis displacement distances were larger in the bowing group (both $p < 0.01$). Strong positive correlations were found between the horizontal head tilt angle and head spacing, spatial head-neck angle and y-axis displacement distance (all $r_s > 0.89$, $p < 0.01$).* **Conclusions:** *MIMICS-based FNF parameter measurement accurately describes spatial characteristics post-fracture, providing guidance for FNF treatment and evaluation.*

Keywords: *Femoral neck fracture. Parameter. Femoral head.*

Resumen

Objetivo: *Investigar la aplicación del software MIMICS para medir los parámetros de las fracturas de cuello femoral (FCF) y su importancia clínica.* **Método:** *Se utilizaron datos de tomografía computarizada de 72 pacientes con FCF para reconstruir modelos tridimensionales (3D) utilizando MIMICS. Las FCF se dividieron en grupos valgo e incurvada según el ángulo cabeza-cuello femoral coronal. Una esfera simulada identificó el centro de la cabeza femoral y se estableció un sistema de coordenadas 3D. Se realizaron análisis estadísticos.* **Resultados:** *El grupo valgo mostró un mayor desplazamiento lateral en el eje x y hacia arriba en el eje z (para ambos $p < 0.01$). Las distancias de desplazamiento medial en el eje x y hacia abajo en el eje z fueron mayores en el grupo de fracturas incurvadas (para ambos $p < 0.01$). Se encontraron fuertes correlaciones positivas entre el ángulo de inclinación horizontal de la cabeza y el espaciamiento de la cabeza, el ángulo espacial cabeza-cuello y la distancia de desplazamiento en el eje y (para todos $_{rs} > 0.89$ y $p < 0.01$).* **Conclusiones:** *La medición de los parámetros de las FCF basada en MIMICS describe con precisión las características espaciales posteriores a la fractura, proporcionando orientación para el tratamiento y la evaluación de las FCF.*

Palabras clave: *Fractura de cuello femoral. Parámetros. Cabeza femoral.*

***Correspondence:**
Feng Liu
E-mail: fengliu1773@163.com

Date of reception: 18-04-2024
Date of acceptance: 19-10-2024
DOI: 10.24875/CIRU.24000222

Cir Cir. 2026;94(2):137-148
Contents available at PubMed
www.cirugiaycirujanos.com

Introduction

Femoral neck fractures (FNFs) are common limb fractures, accounting for approximately 3.6% of all fractures[1]. They are a major public health problem as they are associated with serious medical and social problems[2], as well as having high incidence[3], disability[4,5] and mortality rates[6]. At present, FNFs are generally classified based on pre-operative hip X-ray images, which accordingly determine their treatment selection and prognostic prediction[7].

Previous studies may have only used traditional X-rays for imaging evaluation, without utilising more advanced imaging techniques, such as computed tomography (CT) and magnetic resonance imaging, which may limit a comprehensive understanding of fracture conditions[8]. In addition, existing studies may have only described the imaging findings and not conducted an in-depth analysis of the correlations between these imaging features and clinical outcomes, resulting in a lack of specific guidance for clinicians from imaging results when formulating treatment plans. Moreover, some studies have only described imaging features without conducting quantitative analysis, such as angle or distance measurement on fracture images, thus restricting the accurate evaluation of imaging results[9,10]. On this basis, it is difficult to obtain standard anteroposterior (AP) and lateral views of the pelvis and hip in patients with FNF who often have flexion and external rotation deformities in their affected limbs. MIMICS is a highly integrated and easy-to-use three-dimensional (3D) image generation, editing, and processing software package, which can be used to generate 3D reconstructed images of a patient's anatomy to guide the assessment of the condition and the selection of treatment options. In the field of orthopedics, clinicians use MIMICS software to read CT data directly and visualize the reconstruction of skeletal structures in 3D based on greyscale values. In this way, models with 3D structures for different cases can be obtained, which is a helpful guide for understanding some cases of typical and complex fractures or bone tumors.

The present study analyses in depth the correlations between imaging features and clinical outcomes and conducts a quantitative analysis using more advanced imaging techniques to understand and evaluate the imaging manifestations of FNFs comprehensively and accurately; this can further guide treatment selection, intraoperative reduction, and prognostic prediction of femoral head-preserved treatment.

Method

General data

This study retrospectively collected 72 patients who underwent treatment for FNFs (Garden types I-IV) in our hospital between January 2014 and July 2023. The causes of traumas were traffic accidents (n = 4) and accidental falls (n = 68). All the patients were diagnosed as fresh FNFs. The inclusion criteria were as follows: (1) patients aged > 18 years; (2) patients diagnosed with FNFs by imaging; (3) patients with good communication skills, cooperative willingness, and an ability to understand research procedures and requirements, and who voluntarily signed an informed consent form and participated in the study. The exclusion criteria were as follows: (1) hip dysplasia or rheumatoid arthritis; (2) varus and valgus deformity of the hip; (3) avascular necrosis of the femoral head (ANFH); (4) old FNFs or pathological fractures; (5) long-term alcohol consumption or hormone use; (6) unequal length of the lower limbs and uneven thickness of the femur caused by various reasons; (7) basal FNFs.

Research methods

The CT data (Siemens Healthineers, Erlangen) of the patients were imported into MIMICS for multi-parameter measurement. To facilitate mirror registration, the patients were positioned with healthy lower limbs in the neutral position, the patella facing forward, and the toes straight in midline despite no strict restrictions on the position of the affected limbs. At the same level of the anterior superior iliac spine (ASIS), the pelvis was not tilted. The line connecting the ASIS was parallel to the line connecting the ischial tuberosity.

FNF grouping

Preoperatively, 3D images of the bilateral proximal femur were reconstructed through MIMICS based on CT data (Fig. 1). Using a simulated sphere, the center of the femoral head (CFH) on the healthy side was located, and the size and center of the simulated sphere were calibrated in coronal, horizontal and sagittal planes (Fig. 2). The proximal femur on the affected side was mirrored (Fig. 3). The healthy and

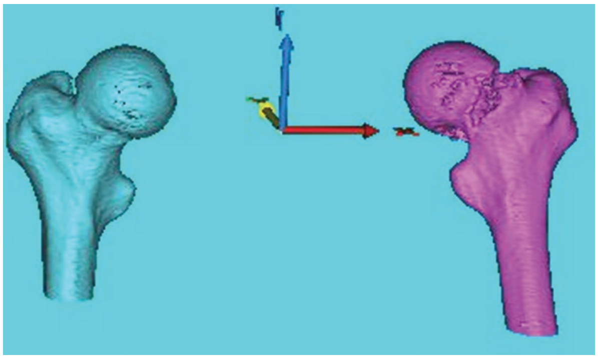

Figure 1. *Dimensional reconstructed radiography of the bilateral proximal femur.*

mirrored affected femoral trochanter and proximal shaft were preliminarily registered using the registration module in MIMICS, followed by calibration of the mask overlap in the coronal, horizontal and sagittal planes by manual rotation and translation to improve accuracy (Fig. 4). The simulated sphere on the healthy side was replicated proportionally to preliminarily locate the CFH on the mirrored affected side, and the simulated sphere was fine-tuned and calibrated according to the mask movement in the three planes on the mirrored affected side (Fig. 5). Using the center of gravity function, the 3D coordinates of the cross-sectional centroid of the base of the femoral neck were located and marked (Fig. 6). Finally, the centroid was connected to the CFH on the healthy and mirrored affected sides in the coronal plane, respectively, to generate a femoral head-neck angle in the coronal plane. Upward opening angles were regarded as valgus angles (the line connecting the CFH on the mirrored affected side and the centroid of the base of the femoral neck was above that connecting the CFH on the healthy side and the centroid) and classified into the valgus group; on the contrary, downward opening angles were classified into the bowing group (Figs. 7 and 8).

Measurement of the CFH displacement

Based on the simulated sphere, the coordinate systems of the CFHs on the healthy and mirrored affected sides were recorded. The spatial displacement of the CFH after FNFs was described by aligning the 3D coordinates of the CFH on the mirrored affected side to the 3D coordinates on the healthy side (Fig. 9).

Measurement of horizontal head tilt angle at the CFH displacement

With the centroid of the base of the femoral neck as the vertex, the CFH on the mirrored affected and healthy sides in the same horizontal plane was connected, and the horizontal head tilt angle after FNFs was measured (Fig. 10).

Measurement of head-neck distance, head spacing and spatial head-neck angle

The distance between the centroid of the base of the femoral neck and the CFH was measured as the head-neck distance, and the distance between the CFHs on the healthy and mirrored affected sides as the head spacing. In addition, the spatial head-neck angle (∠A) was calculated using the unknown length of the three sides according to the cosine theorem and the formula ACOS ([$AB^2 + AC^2 - BC^2$)/2*AB*AC)*180/PI() in Excel (Fig. 11).

Statistical methods

Data were statistically analyzed using the Statistical Package for the Social Sciences 24.0. Enumeration data were expressed as rates and compared by the Chi-squared test. Measurement data were described as mean ± standard deviation and tested for normality. The measurement data conforming to a normal distribution were compared with the independent sample *t*-test to investigate the therapeutic effect at different time points and its interaction with treatment. Non-normally distributed measurement data were analyzed using the Friedman test. Pearson correlation analysis was performed to verify the correlations among coefficients. A significance level of $p < 0.05$ was applied to all statistical tests and considered statistically significant.

Results

Measured data

A total of 72 patients were recruited in this study, including 30 patients in the valgus group and 42 patients in the bowing group; there were 35 (48.61%) men and 37 (51.39%) women, with an age range of 21-89 years (average age, 63.40 ± 12.88 years). Among them, 36 (50%) patients suffered from

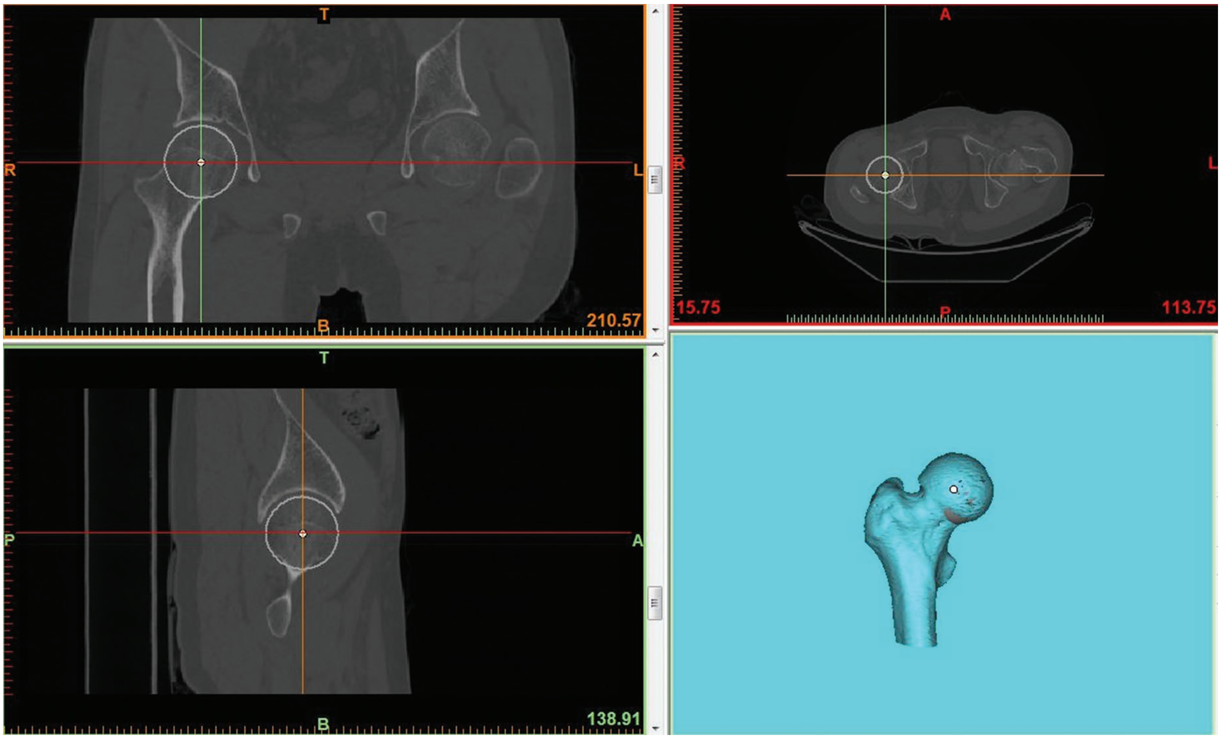

Figure 2. *Determination of the healthy femoral head center and calibrated in coronal, horizontal, and sagittal planes.*

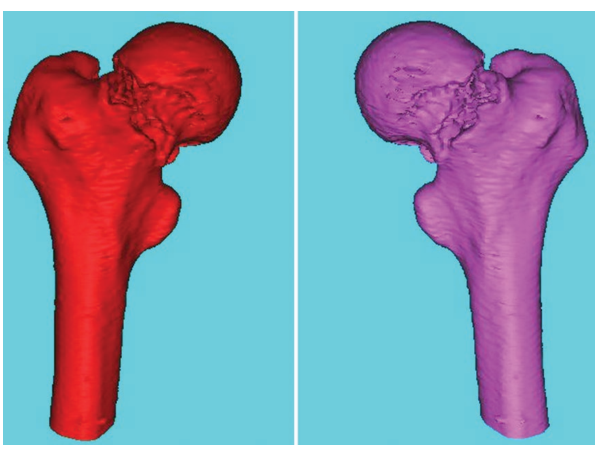

Figure 3. *Purple is the affected side, red is the mirrored affected side.*

left-sided FNFs and 36 (50%) experienced right-sided FNFs. Thirty (41.67%) patients were classified as stable type (Garden types I/II) and 42 (58.33%) as unstable type (Garden types III/IV).

After FNFs, the CFH presented lateral displacement in 37 (51.39%) patients and medial displacement in 35 (48.61%) patients, with x-axis displacement (mm) of −11.13-15.42 (0.12 ± 5.79) (the medial or lateral displacement of the CFH after FNFs was related to the fractured side; therefore, for computational convenience, a positive number was specified in the overall samples to indicate medial displacement and a negative number to represent lateral displacement). Upward displacement occurred in 24 (33.33%) patients and downward displacement in 48 (66.67%), with z-axis displacement (mm) of −19.75-4.22 (−6.81 ± 7.07) (a positive number indicated upward displacement and a negative number represented downward displacement). Posterior displacement occurred in 71 (98.61%) patients and anterior displacement in 1 (1.39%) patient, with y-axis displacement (mm) of −4.97-31.29 (12.26 ± 8.01) (a positive number represented posterior displacement and a negative number indicated anterior displacement).

The horizontal head tilt angle was −14.79°-74.94° (31.49° ± 20.05°) (a positive number indicated posterior tilt and a negative number represented anterior tilt). Anterior tilt occurred in 2 patients (1 patient in the valgus group and 1 patient in the bowing group), and posterior tilt was found in 70 (97.22%) patients. The head-neck distance (mm) was 25.33-41.99 (31.55 ± 3.57) on the healthy side and 19.10-39.54 (28.22 ± 4.37) on the affected side. The head spacing (mm) was 2.18-34.29 (16.60 ± 8.32). The spatial head-neck angle was measured as 2.87°-73.33° (31.16° ± 17.09°) (Table 1).

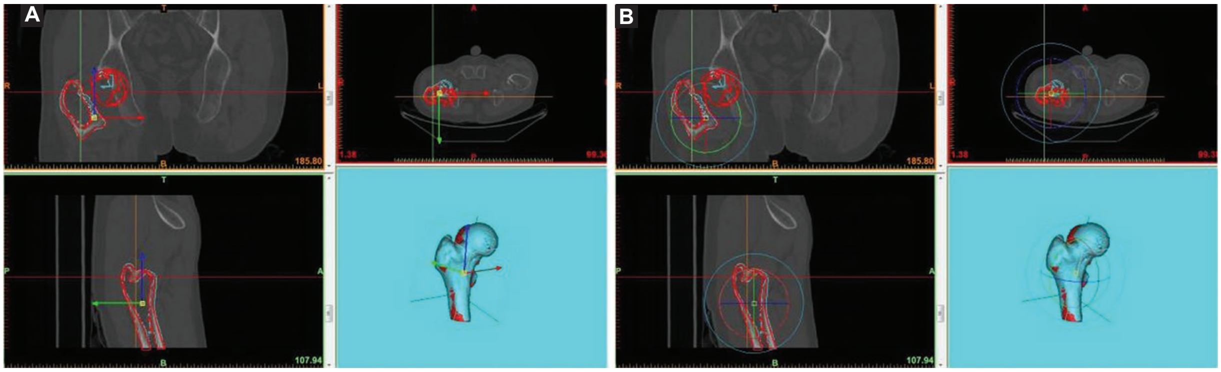

Figure 4. *The trochanter of femur was registered by displacement and rotation.* **A:** *displacement function,* **B:** *rotation function. Red is the mask of mirrored affected side, blue is mask of healthy side, manual registration on mask can adjust the 3D registration accurately.*

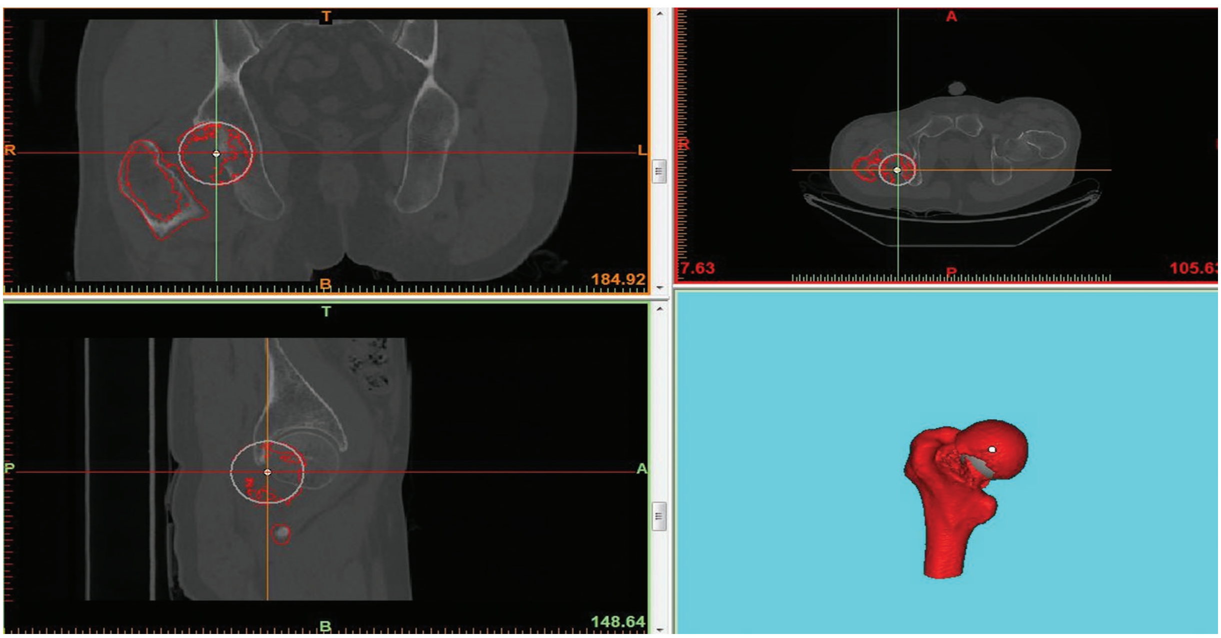

Figure 5. *Determination the center of the mirrored affected femoral head.*

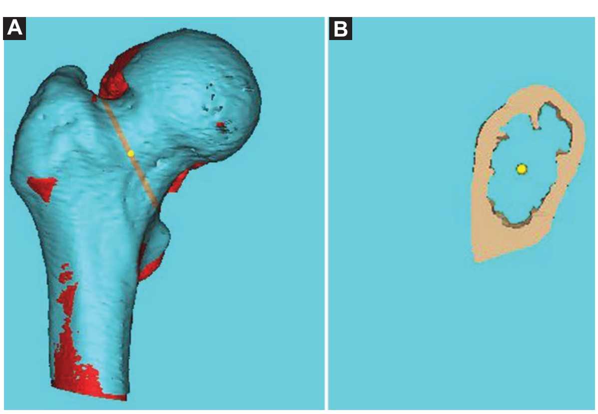

Figure 6. *Determination of the base center of gravity of the femoral neck.* **A:** *three-dimensional view of the basilar center of gravity of the femoral neck,* **B:** *cross-sectional view of the basilar center of gravity of femoral neck.*

Inter-group statistical results

The age of onset in the bowing group was 38-89 years (66.07 ± 12.71 years), which was higher than the 21-88 years (59.67 ± 12.37 years) in the valgus group, and the difference was statistically significant ($p < 0.05$). However, comparisons of gender and involved sides showed no statistical differences between the two groups ($p > 0.05$). The incidence of unstable FNFs was higher in the bowing group compared with the valgus group (97.67% vs. 3.33%), with a statistically significant difference ($p < 0.01$).

According to the analysis of CFH displacement, the valgus group was more prone to lateral displacement

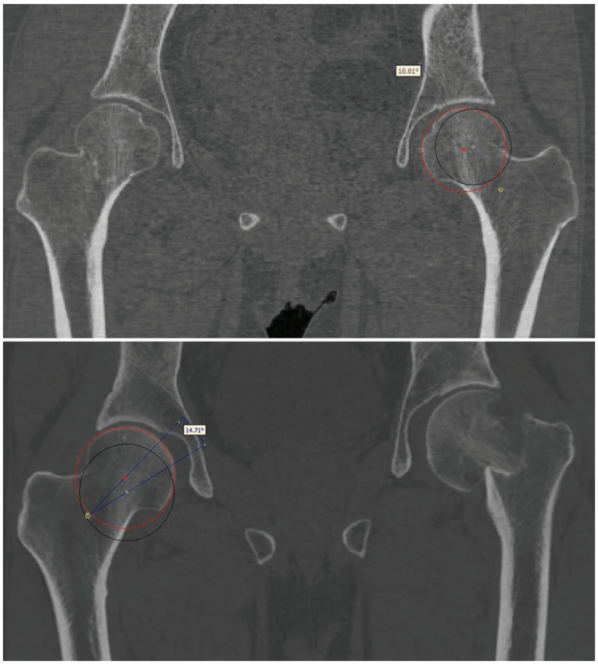

Figure 7. *Group of head-up/head-down. Black is the mirrored image of the affected femoral head, red if the healthy side, and yellow is the base center of mass of the femoral neck.*

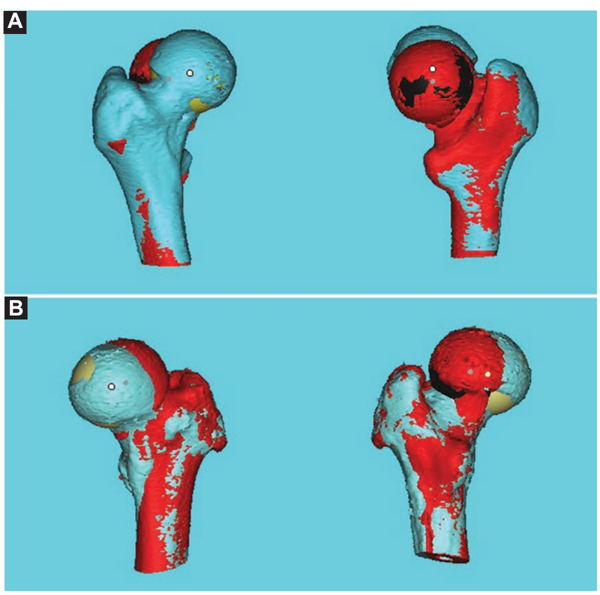

Figure 8. A: *head-down group 3D image,* **B:** *head-up group 3D image. Red is the mirrored affected side.*

(100%) and upward displacement (80%), whereas the bowing group was more prone to medial displacement (83.33%) and downward displacement (100%), presenting statistically significant differences ($p < 0.01$). Both groups exhibited posterior displacement, 100% in the valgus group and 97.62% in the bowing group, without statistically significant differences ($p > 0.05$).

Based on the comparisons of three-axis displacement distances, it was found that the x-axis displacement distance (mm) was 0.10-11.82 (4.83 ± 3.29) in the valgus group and 0.05-15.42 (4.17 ± 3.94) in the bowing group, with no statistical difference ($p > 0.05$). The y-axis displacement distance (mm) was 1.94-31.29 (16.52 ± 7.47) in the bowing group, which was larger than the 0.37-18.84 (6.30 ± 3.86) in the valgus group, with a statistically significant difference ($p < 0.01$). The z-axis displacement distance (mm) was larger in the bowing group compared with the valgus group (4.20-19.75 [–12.06 ± 3.91] vs. 0.25-6.08 [1.66 ± 1.51]), and the difference was statistically significant ($p < 0.01$).

The measurement of the coronal head-neck angle revealed that the bowing angle (1.91°-43.24° [23.90° ± 10.84°]) was larger than the valgus angle (1.64°-22.12° [8.44° ± 5.20°]), with a statistically significant difference ($p < 0.01$). Considering only the degree but not the direction, the horizontal head tilt angle was 8.86°-74.94° (43.05° ± 15.78°) in the bowing group, which was larger than the 0.08°-44.45° (17.53° ± 11.29°) in the valgus group, with a statistically significant difference ($p < 0.01$). In 3D space, the head spacing (6.40-34.29 [22.13 ± 5.87] mm) and spatial head-neck angle (9.57°-73.33° [42.39° ± 12.72°]) in the bowing group were larger compared with the valgus group (2.18-20.07 [8.86 ± 3.80] mm, 2.87°-35.45° [15.44° ± 6.95°]), with statistically significant differences ($p < 0.01$) (Table 1).

Correlation analysis

To explore the correlations among multiple variables, a correlation matrix was constructed, revealing significant correlations between horizontal head tilt angle, head spacing, spatial head-neck angle, coronal head-neck angle (valgus or bowing angle), y-axis displacement distance and z-axis displacement distance ($p < 0.01$). Extremely strong positive linear correlations were detected between horizontal head tilt angle and head spacing ($r_s = 0.895$, $p < 0.01$), spatial head-neck angle ($r_s = 0.907$, $p < 0.01$), and y-axis displacement distance ($r_s = 0.943$, $p < 0.01$), as shown in table 2.

Discussion

Standardization of FNF classification

The common classifications for FNFs include the Garden classification, Pauwels classification, Linton

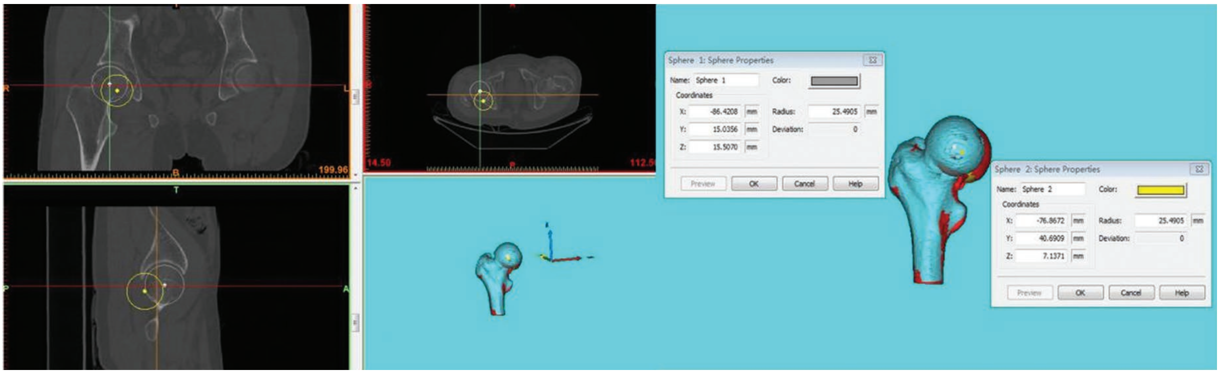

Figure 9. *Spatial displacement of the femoral head. X means internal and external shift, Y means forward and backward shift, and Z means up and down shift.*

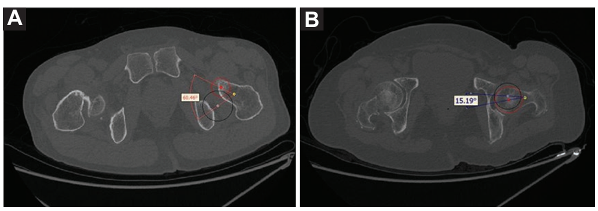

Figure 10. *Measurement of horizontal head tilt angle.* **A:** *posterior tilt angle,* **B:** *anterior tilt angle. Black is the mirrored image of the affected femoral head. Red is the healthy side, and yellow is the base center of gravity of the femoral neck.*

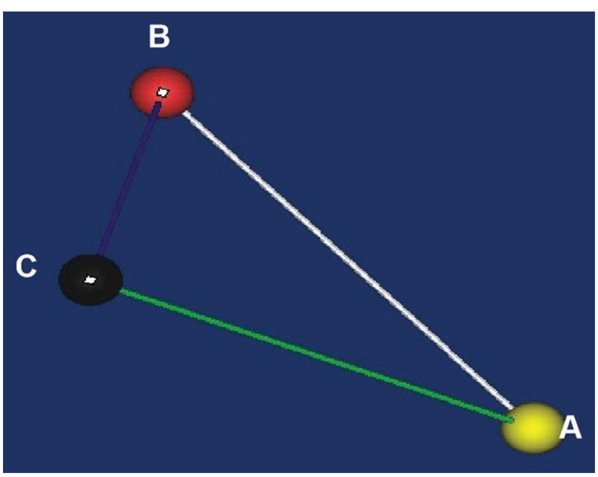

Figure 11. *Measurement of head-neck distance, head spacing, and spatial head-neck angle. AB and AC are the head spacing, and BC is the head-neck distance.*

classification and AO classification, all of which are based on X-ray image reading. However, patients with FNFs often have deformities, such as flexion, shortening, and external rotation, and are also limited by the uncertainty of distance, angle, and center during X-ray projection. This causes difficulty in capturing standard AP pelvic and hip radiographs, which are prone to missed diagnosis and misdiagnosis[11]. At present, the Garden classification is commonly used in clinical practice[12], with Type I as an incomplete fracture, Type II as a complete fracture without significant displacement, Type III as a complete fracture with partial displacement, and Type IV as a complete fracture with complete displacement. Some scholars believe that through CT and 3D reconstruction, incomplete fractures do not actually exist[13]; therefore, they classify impacted fractures as Garden Type I. Du et al.[14] identified six cases of incomplete fractures out of patients with Garden Type I fractures based on X-ray imaging and then confirmed three cases as incomplete fractures through CT and 3D reconstruction. Consequently, they believe that incomplete fractures do exist, but the incidence rate is relatively low. Du et al.[15] have found after CT scans of 50 individuals with normal hips and the application of MIMICS mirror registration that the external morphology of the bilateral proximal femur is highly symmetrical, and the error generated by MIMICS registration is $\leq$ 1 mm. In the present study, no incomplete fractures were detected in 28 patients with Garden type I FNFs based on MIMICS reconstruction and registration, a review in the coronal, horizontal, and sagittal planes, as well as analysis of CFH displacement distance, horizontal tilt angle, and head spacing. In addition, in distinguishing Garden Type III, IV, and another Pauwels type based on the angle generated by fracture lines commonly used in clinical practice, X-ray imaging has a high misdiagnosis rate in that the fracture lines displayed on X-ray images are actually irregular projections of the fracture surface in the coronal plane on CT. Moreover, all types of FNFs are based on AP X-ray images of the hip, without considering lateral displacement. Our study demonstrates that the so-called stable types (I/II) in the Garden

Table 1. Comparative analysis of measured results

Factor	Total	Valgus group	Bowing group	p	χ²	t
Case	72	30	42			
Age	63.40 ± 12.88	59.67 ± 12.37	66.07 ± 12.71	0.037		2.132
Gender				0.217	1.527	
Male	35 (48.61)	12 (40.00)	23 (54.76)			
Female	37 (51.39)	18 (60.00)	19 (45.24)			
Side				0.151	2.075	
Left	36 (50.00)	18 (60.00)	18 (42.86)			
Right	36 (50.00)	12 (40.00)	24 (57.14)			
Garden classification				< 0.001	53.024	
Stable type						
I	28 (38.89)	27 (90.00)	1 (2.38)			
II	2 (2.78)	2 (6.67)	0 (0.00)			
Unstable type						
III	26 (36.11)	1 (3.33)	25 (59.52)			
IV	16 (22.22)	0 (00.00)	16 (38.10)			
X-axis				< 0.001	48.649	
Medial displacement (n)	35 (48.61)	0 (0.00)	35 (83.33)			0.754
Lateral displacement (n)	37 (51.39)	30 (100.00)	7 (16.67)			
Displacement (mm)	0.12 ± 5.79	−4.83 ± 3.29	3.12 ± 4.83			
Displacement distance (mm)		4.83 ± 3.29	4.17 ± 3.94	0.453		
Y-axis				1.000*		
Anterior displacement (n)	1 (1.39)	0 (0.00)	1 (2.38)			8.185
Posterior displacement (n)	71 (98.61)	30 (100.00)	41 (97.62)			
Displacement (mm)	12.26 ± 8.01	6.30 ± 3.86	16.52 ± 7.47	< 0.001		
Z-axis				< 0.001	50.400	
Upward displacement (n)	24 (33.33)	24 (80.00)	0 (00.00)			
Downward displacement (n)	48 (66.67)	6 (20.00)	42 (100.00)			15.677
Displacement (mm)	−6.81 ± 7.07	0.55 ± 2.19	−12.06 ± 3.91	< 0.001		
Valgus angle	-	8.44° ± 5.20°	-			
Bowing angle	-	-	23.90° ± 10.84°			
Horizontal head tilt angle	31.49° ± 20.05°	16.69° ± 12.54°	42.06° ± 17.61°			
Head-neck distance/healthy side (mm)	31.55 ± 3.57	31.20 ± 3.82	31.80 ± 3.40			
Head-neck distance/affected side (mm)	28.22 ± 4.37	28.09 ± 4.56	28.31 ± 4.28			
Head spacing	16.60 ± 8.32	8.86 ± 3.80	22.13 ± 5.87			
Spatial head-neck angle	31.16° ± 17.09°	15.44 ± 6.95	42.39 ± 12.72			
Valgus angle/Bowing angle (°)		8.44° ± 5.20°	23.90° ± 10.84°	< 0.001		−7.230
Horizontal head tilt angle(°)		17.53° ± 11.29°	43.05° ± 15.78°	< 0.001		−8.000
Head spacing		8.86 ± 3.80	22.13 ± 5.87	< 0.001		−11.629
Spatial head-neck angle		15.44° ± 6.95°	42.39° ± 12.72°	< 0.001		−11.528

*Fisher's exact probability test was applied when n > 40 and expected cell count < 1 (a minimum cell expectation of 0.42) in the Chi-square test.

classification may not have significant displacement and be stable on the AP view, but may have significant displacement and be unstable on the lateral view. Furthermore, the 3D spatial changes in the head-neck angle, stretching distance, and shortening distance confirm that FNFs are complex 3D spatial fractures and cannot be classified solely using a two-dimensional (2D) model. The application of a 2D classification in guiding and evaluating the reduction and prognosis of 3D fractures is not accurate.

Table 2. Pearson product-moment correlation coefficient

Correlation factor	Horizontal head tilt angle	Head spacing	Coronal head-neck angle	Spatial head-neck angle	Y-axis displacement distance	Z-axis displacement distance
Horizontal head tilt angle	1					
Head spacing	0.895**	1				
Coronal head-neck angle	0.428**	0.688**	1			
Spatial head-neck angle	0.907**	0.975**	0.713**	1		
Y-axis displacement distance	0.943**	0.915**	0.408**	0.895**	1	
Z-axis displacement distance	0.561**	0.784**	0.818**	0.787**	0.558**	1

**Significantly correlated at the 0.01 level (two-tailed).

Some scholars[16] hold the view that impacted fractures belong to stable fractures and can be treated conservatively, which is inaccurate. Among the 28 patients with impacted fractures in our study, 13 (46.43%) of the horizontal head tilt angles and 8 (28.57%) of the spatial head-neck angles were > 20°. One study[17] has shown that the failure rate of internal fixation is 13.6% when the pre-operative posterior tilt angle of the hip is < 20°, and the failure rate of internal fixation is as high as 56% with the posterior tilt angle > 20°. Therefore, defining impacted fractures as Garden Type I is not accurate, and conservative treatment is not the first choice. It has also been demonstrated that given the high failure rate in patients with pre-operative anterior tilt angle > 10°, initial hip replacement is recommended for this subgroup of elderly patients[18]. As a result, these patients should be actively treated by surgery, such as hip replacement, with the main goal of actively correcting the (anterior) posterior tilt angle rather than *in situ* fixation.

Anatomical characteristics of FNFs

Regarding the morphology of FNFs on CT, the valgus group was dominated by valgus-impacted FNFs, with laterosuperior impaction, medioinferior impaction or abduction, separation, and displacement in the coronal plane; the bowing group mostly comprised varus distraction fractures, presenting laterosuperior distraction and medioinferior angular deformity in the coronal plane. In the coronal plane, the bowing angle was significantly larger than the valgus angle, indicating that the angular displacement of the CFH in the coronal plane after FNFs was significantly larger in the bowing group than in the valgus group. Yamamoto et al.[19] have shown that a posterior tilt angle > 20° on a CT image is correlated with complications such as ANFH. In our study, the number of patients with a head tilt angle > 20° in the horizontal plane measured by CT was greater than that in the valgus group, suggesting that when head-preserving surgery is chosen, the bowing group is more prone to complications, such as internal fixation failure and ANFH. In addition, retinacular arterial damage and venous drainage of the femoral neck and head may lead to higher failure rates in patients with a more pronounced tilt[18,20]. The failure of internal fixation that requires a salvage hip replacement is a severe complication in elderly patients, as it is less effective compared with the initial hip replacement[21,22]. Moreover, according to the research on the blood supply and anatomy of the femoral head, the lateral ascending cervical artery supplies between 2/3 and 3/4 of the blood supply to the femoral head, including the blood supply to the weight-bearing area, and the medial ascending cervical artery supplies between 1/4 and 1/3 of the blood supply to the femoral head[23]. Based on the morphological characteristics of both groups, laterosuperior distraction displacement in the bowing group and laterosuperior impaction displacement in the valgus group, the bowing group is more likely to cause damage to the lateral ascending cervical artery. Therefore, blood supply should be preserved in patients undergoing initial hip replacement.

FNFs are mainly caused by a head-neck imbalance, rather than a neck-shaft imbalance (except basal FNFs). The neck-shaft angle is the intersection angle between the proximal femoral axis and the femoral neck axis. In cases of FNFs, particularly subcapital FNFs, the neck-shaft angle is not actually changed, but rather the anatomical relationship between the femoral neck axis and the CFH changes. Under normal conditions, the femoral neck axis, where the base of the femoral neck is located, should be collinear with the CFH. When FNFs (except basal FNFs) occur, the CFH is deviated from the femoral neck axis. The CFH displacement after FNFs in the coronal, horizontal and sagittal planes can be obtained through collecting pre-operative CT data from patients, reconstructing and mirroring the affected proximal femur based on MIMICS, registering the healthy proximal femur and utilising the 3D coordinates of CFHs on both healthy and mirrored affected sides. Our data confirmed that the fracture displacement was more obvious, the stability was worse and the injury was more severe in the bowing group.

Clinical significance of parameter measurement based on MIMICS

For a more accurate description of 3D spatial CFH displacement after FNFs, reference points are required to accurately describe the displacement distances and angle changes of the CFH in 3D space. Du et al.[14] used small concavities of the bilateral femoral head as reference points, but the concavity of the affected femoral head needed to be manually located using a horizontal mask after MIMICS mirror imaging. The accuracy was not high due to factors such as mask errors and single-plane limitations. Our study located the centroid of the base of the bilateral femoral neck after registration through the center of gravity function of MIMICS. Although the medullary cavity of the femoral neck was irregular under actual conditions, the centroid of the medullary cavity was equivalent to the center in ideal conditions. Therefore, based on the theory thatthe external morphology of the bilateralproximal femurs is highly symmetrical[15], the mirror-aligned bilateralfemoral neck base centroids overlap. The centroid was connected to the CFH on the healthy and affected sides, respectively, to generate a head-neck angle in the coronal plane. Patients with the connecting line of the affected side above were classified into the valgus group; otherwise, patients were classified into the bowing group. The differences between the two groups were statistically analyzed. Under the same external force, elderly patients are prone to more severe fractures. Compared with the Garden and Pauwels classifications based on X-ray imaging, pre-operative inter-group parameter measurement through MIMICS based on CT images is simpler and more accurate. There were statistically significant differences between the two groups in many key parameters. A personalized surgical plan was developed preoperatively based on the distinct anatomical characteristics of FNFs in the two groups. For lateral tilt angles in particular, appropriate intraoperative reduction techniques, such as hip flexion, internal rotation, and even Kirschner wire prying according to preoperatively measured parameters, were needed to correct posterior tilt and rotation deformities; these aimed to achieve an accurate reduction in multiple planes and 3D space, rather than a simple 2D reduction on AP and lateral views. Postoperatively, CT was reviewed, re-reconstruction/registration was performed based on MIMICS, and the spatial reduction effect was accurately evaluated.

Horizontal tilt angle

Alho et al.[24] have discovered a correlation between the posterior tilt angle of FNFs and internal fixation failure. Shin et al.[25] measured the posterior tilt angle based on pre-operative and post-operative X-ray imaging and confirmed the correlation between the posterior tilt angle and femoral head necrosis. The above measurements are all based on X-ray imaging, and the accuracy needs to be further verified. There is currently no unified standard for the definition and measurement method of the posterior tilt angle. The conventional X-ray-based measurement is achieved by supine horizontal projection[17], which is limited by factors such as patients' pre-operative position, uncertainty of projection center, and interference from 2D images, resulting in poor measurement accuracy. Liu et al.[26] have found by examining X-ray supine horizontal measurements that when the pre-operative posterior tilt angle is > 15°, the incidence of complications associated with internal fixation for FNFs is higher. However, Yamamoto et al.[19] believe that X-ray measurement is not accurate, and for some patients without significant displacement on X-ray imaging, CT still displays a posterior tilt angle > 20°. With the widespread application of CT technology and the emergence of MIMICS, the measurement method for the posterior tilt angle has become more extensive and accurate. In the study by Du et al.[14], the small concavities of the bilateral femoral head on the healthy and mirrored affected sides were, respectively, connected to their CFHs, and the angle between the two spatial straight lines was defined as the posterior tilt angle, which is limited to Garden Types I and

II only. This method not only theoretically ensures that the CFHs on the healthy and affected sides are in the same plane but also ensures the intersection of the two lines. However, Garden Types III and IV, with significant displacement of the femoral head, were not studied in their research. Zhan et al.[27] defined the posterior tilt angle as the angle generated by connecting the CFHs on the healthy and affected sides to the centroid of the entire femoral neck, respectively. The limitation of this study lies in the fact that, except for subcapital FNFs, the centroids of the registered intact femoral neck on the healthy side and the fractured femoral neck on the affected side may not necessarily coincide. Therefore, the above studies can only be theoretically applicable to Garden Types I and II FNFs. Moreover, the so-called posterior tilt angle defined in the two studies is a spatial 3D angle, rather than a conventional planar (coronal, horizontal, sagittal) angle. MIMICS has no function for spatial angle measurement. Using the 2D angle measurement tool of MIMICS to measure an unconventional and non-planar angle in 3D space will result in larger measurement errors as the angle increases. The spatial head-neck angle measured in our study was a spatial angle calculated using mathematical formulae based on known trilateral lengths, which was not in any plane on CT. In this study, the valgus or bowing angle was a projection angle of the spatial head-neck angle in the coronal plane on CT, while the horizontal head tilt angle was the projection of this angle in the horizontal plane on CT. According to the single-factor correlation analysis, an extremely strong positive correlation was detected between the horizontal head tilt angle and the spatial head-neck angle. This study used the spatial head-neck angle and horizontal head tilt angle to represent posterior tilt angle in previous studies separately but did not define them as posterior tilt angle because of the presence of anterior head tilt in our study. Some scholars[15] believe that after violent force acts on the femoral head, the anatomical characteristics of the hip and proximal femoral neck, as well as axial forces, can cause posterior head tilt. However, no relevant literature has been found to explain the anterior tilt of the head after FNFs. Therefore, our study suggests that the definition of posterior head tilt is not accurate. Furthermore, due to the common phenomenon of posterior head tilt in FNFs, it is indicated that the front part of the femoral neck is the tension side, so cannulated screws should not be tilted backwards.

Limitations

Inevitably, there were several limitations in this study. First, the limited sample size and single-center nature of this study reduce the persuasiveness of this investigation. Second, this study did not perform subgroup analyses, which may ignore differences in imaging performance in different FNF populations. Furthermore, all the patients in this study were fresh FNFs, so the results may not apply to patients with old or pathologic FNFs.

Conclusions

The spatial parameter measurement through MIMICS software based on CT data of FNFs can more accurately describe the spatial characteristics after FNFs, which is conducive to standardizing fracture classification and providing a theoretical basis for establishing a more accurate and effective spatial 3D classification. Moreover, based on the characteristics of pre-operative 3D parameters, it can help surgeons choose appropriate treatment methods, develop personalized surgical plans, improve reduction quality, and reduce post-operative complications. Large-sample, multicenter studies should be performed in the future to validate our findings.

Funding

The authors declare that they have not received funding.

Conflicts of interest

The authors declare no conflicts of interest.

Ethical considerations

Protection of human subjects and animals. The authors declare that the procedures followed complied with the ethical standards of the responsible human experimentation committee and adhered to the World Medical Association and the Declaration of Helsinki. The procedures were approved by the Institutional Ethics Committee.

Confidentiality, informed consent, and ethical approval. The authors have followed their institution's confidentiality protocols, obtained informed consent from all patients, and secured approval from the

Ethics Committee. SAGER guidelines have been followed as applicable to the nature of the study.

Declaration on the use of artificial intelligence. The authors declare that no generative artificial intelligence was used in the writing or creation of the content of this manuscript.

References

1. Wu M, Zhuang W, Zheng J, Li X, Chen M, Fan X, et al. Computerized navigation system assisted the placement of the cannulated screw and internal fixation for the treatment of femoral neck fractures. Chin J Clin Anat. 2021;39:454-9.
2. Naseri A, Shojaeefard E, Bakhshayeshkaram M, Dabbaghmanesh MM, Heydari ST, Talezadeh P, et al. Hip structural analysis, trabecular bone score, and bone mineral density in post-menopausal women with type-2 diabetes mellitus: a multi-center cross-sectional study in the South of Iran. Arch Osteoporos. 2023;18:98.
3. Jaya Raj J, Kow RY, Ganthel Annamalai K, Kunasingh DE, Panicker GK, Lim BC, et al. Outcomes of femoral neck fractures in young patients and the factors associated with complications: a multicenter study from Malaysia. Cureus. 2021;13:e18110.
4. Bartels S, Gjertsen JE, Frihagen F, Rogmark C, Utvag SE. Low bone density and high morbidity in patients between 55 and 70 years with displaced femoral neck fractures: a case-control study of 50 patients vs 150 normal controls. BMC Musculoskelet Disord. 2019;20:371.
5. Ganhão S, Guerra MG, Lucas R, Terroso G, Aguiar F, Costa L, et al. Predictors of mortality and refracture in patients older than 65 years with a proximal femur fracture. J Clin Rheumatol. 2022;28:e49-55.
6. Muñoz-Garach A, García-Fontana B, Muñoz-Torres M. Nutrients and dietary patterns related to osteoporosis. Nutrients. 2020;12:1986.
7. Thevenot J, Hirvasniemi J, Pulkkinen P, Määttä M, Korpelainen R, Sarrakkala S, et al. Assessment of risk of femoral neck fracture with radiographic texture parameters: a retrospective study. Radiology. 2014;272:184-91.
8. Beyaz S, Açıcı K, Sümer E. Femoral neck fracture detection in X-ray images using deep learning and genetic algorithm approaches. Jt Dis Relat Surg. 2020;31:175-83.
9. Shitova AD, Kovaleva ON, Olsufieva AV, Gadzhimuradova IA, Zubkov DD, Kniazev MO, et al. Risk modeling of femoral neck fracture based on geometric parameters of the proximal epiphysis. World J Orthop. 2022;13:733-43.
10. Sano K, Homma Y, Shirogane Y, Ishii S, Ito T, Baba T, et al. Acetabular morphological variation in Asian patients with femoral neck fracture: a three-dimensional CT-based study. Injury. 2022;53:2823-31.
11. Sadozai Z, Davies R, Warner J. The sensitivity of CT scans in diagnosing occult femoral neck fractures. Injury. 2016;47:2769-71.
12. Garden RS. Low-angle fixation in fractures of the femoral neck. J Bone Joint Surg Br Vol. 1961;43:647-63.
13. Chen W, Li Z, Su Y, Hou Z, Zhang Q, Zhang Y. Garden type I fractures myth or reality? A prospective study comparing CT scans with X-ray findings in garden type I femoral neck fractures. Bone. 2012;51:929-32.
14. Du C, Shi H, Wang J, Meng T, Ren Q, Xu C, et al. Three-dimensional reconstruction study of the displacement of femoral neck fractures and proposal of modified Garden's classification. J Binzhou Med Univ. 2018;41:161-4.
15. Du CL, Ma XL, Zhang T, Zhang HF, Wang CG, Zhao F, et al. Reunderstanding of garden type I femoral neck fractures by 3-dimensional reconstruction. Orthopedics. 2013;36:820-5.
16. Slobogean GP, Stockton DJ, Zeng B, Wang D, Ma BT, Pollak AN. Femoral neck fractures in adults treated with internal fixation: a prospective multicenter Chinese cohort. J Am Acad Orthop Surg. 2017;25:297-303.
17. Palm H, Gosvig K, Krasheninnikoff M, Jacobsen S, Gebuhr P. A new measurement for posterior tilt predicts reoperation in undisplaced femoral neck fractures: 113 consecutive patients treated by internal fixation and followed for 1 year. Acta Orthop. 2009;80:303-7.
18. Sjöholm P, Sundkvist J, Wolf O, Skoldenberg O, Gordon M, Mukka S. Pre-operative anterior and posterior tilt of garden I-II femoral neck fractures predict treatment failure and need for reoperation in patients over 60 years. JB JS Open Access. 2021;6:e21.00045.
19. Yamamoto T, Kobayashi Y, Nonomiya H. Undisplaced femoral neck fractures need a closed reduction before internal fixation. Eur J Orthop Surg Trauma. 2019;29:73-8.
20. Lazaro LE, Klinger CE, Sculco PK, Helfet DL, Lorich DG. The terminal branches of the medial femoral circumflex artery: the arterial supply of the femoral head. Bone Joint J. 2015;97-b:1204-13.
21. Gojda J, Bartoníček J. The retinacula of Weitbrecht in the adult hip. Surg Radiol Anat. 2012;34:31-8.
22. Frihagen F, Madsen JE, Aksnes E, Bakken HN, Maehlum T, Walloe A, et al. Comparison of re-operation rates following primary and secondary hemiarthroplasty of the hip. Injury. 2007;38:815-9.
23. Wu Q, Lian P, Wang J, Han Y. An anatomical study of avascular necrosis of the femoral head after hip-salvage operation. Chin J Bone Joint. 2015;4:399-403.
24. Alho A, Benterud JG, Ronningen H, Hoiseth A. Prediction of disturbed healing in femoral neck fracture. Radiographic analysis of 149 cases. Acta Orthop Scand. 1992;63:639-44.
25. Shin WC, Moon NH, Jang JH, Jeong JY, Suh KT. Three-dimensional analyses to predict surgical outcomes in non-displaced or valgus impaction fractures of the femoral neck: a multicenter retrospective study. Orthop Traumatol Surg Res. 2019;105:991-8.
26. Liu G, Ji W, Liu J, Jiang H. Analysis of related factors and evaluation of quality of life of osteonecrosis of femoral head after internal fixation of femoral neck fracture. China J Orthop Traumatol. 2008;8:750-7.
27. Zhan H, Ma J, Cui S, Sun L, Wang Y, Bai H, et al. Correlation between three-dimensional measurement of posterior tilt of impacted femoral neck fracture and femoral head necrosis. Chin J Tissue Eng Res. 2023;27:5747-52.